

An Improved Texture Feature Extraction Method for Recognizing Emphysema in CT Images

Shao-Hu Peng* · Hyun-Do Nam**

Abstract

In this study we propose a new texture feature extraction method based on an estimation of the brightness and structural uniformity of CT images representing the important characteristics for emphysema recognition.

The Center-Symmetric Local Binary Pattern (CS-LBP) is first used to combine gray level in order to describe the brightness uniformity characteristics of the CT image. Then the gradient orientation difference is proposed to generate another CS-LBP code combining with gray level to represent the structural uniformity characteristics of the CT image.

The usage of the gray level, CS-LBP and gradient orientation differences enables the proposed method to extract rich and distinctive information from the CT images in multiple directions. Experimental results showed that the performance of the proposed method is more stable with respect to sensitivity and specificity when compared with the SGLDM, GLRLM and GLDM. The proposed method outperformed these three conventional methods (SGLDM, GLRLM, and GLDM) 7.85[%], 22.87[%], and 16.67[%] respectively, according to the diagnosis of average accuracy, demonstrated by the Receiver Operating Characteristic (ROC) curves.

Key Words : Medical image, Chest CT Image, Emphysema, Local Binary Pattern, Feature Extraction

1. Introduction

Due to the advantages of Computed Tomography (CT), CT scans are usually used to examine

pathological changes of tissues inside the human body. However, a large number of images generated by CT scanners require considerable time and effort for the radiologist to diagnose pathological change of the patient. Therefore, in recent years, a number of computer-aided detection (CAD) systems [1-4] have been developed to help the radiologists to diagnose diseases. Using CAD systems to detect lung diseases such as emphysema [5-7] is currently one of the most important fields in the medical image processing.

* Main author : Ph.D. Student, Dankook University
** Corresponding author : Professor, Dankook University
Tel : +82-31-8005-3603, Fax : +82-31-8005-3622
E-mail : hdnam@dankook.ac.kr
Date of submit : 2010. 11. 4
First assessment : 2010. 11. 6
Completion of assessment : 2010. 11. 19

For the CAD systems, feature extraction is one of the most important steps for detecting pathological change regions in the CT images. In past decades, texture features such as the gray level difference method (GLDM), the gray level run-length method (GLRLM), and the spatial gray level dependent method (SGLDM) [8], have been widely used to represent the medical image characteristics which are inaccessible to human observers.

However, experimental results showed that the performances of these algorithms depended on their feature extraction directions [6,7]. To overcome this problem, Peng et al. [6,7] proposed to employ the local binary pattern (LBP) [9] and rotation invariant local binary pattern [10] to extract rich image features in multiple directions. Recently, a modified version of LBP called Center-Symmetric Local Binary Pattern (CS-LBP) was proposed to describe local image features using a short histogram and a simple computation [11].

In this paper, a new texture feature extraction method is proposed which describes the local image uniformity of brightness and structure based on the CS-LBP.

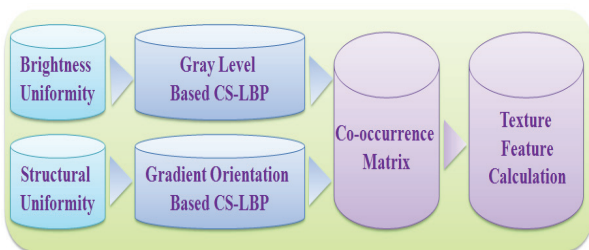


Fig. 1. Texture feature extraction based on brightness and structural uniformity

- First, as shown in Fig. 1, the gray level based CS-LBP is used to represent the brightness uniformity of the local image feature. Due to the gray value comparison of the center-symmetric pixel pairs of CS-LBP, this

feature can be used as a measure of brightness uniformity.

- Second, the gradient orientation based CS-LBP is proposed to further estimate the structural uniformity of the local image feature. Since the gradient orientation can describe the image local structure, it is a good measure to estimate the local uniformity of the image structure.
- Finally, a co-occurrence matrix based on both features is constructed for texture feature calculation.

Four new texture features, Brightness Variance Emphasis (BVE), Brightness Uniformity Emphasis (BUE), Structure Variance Emphasis (SVE) and Structure Uniformity Emphasis (SUE) are proposed for representing the brightness and structural uniformity of the local image feature. Since these features are extracted in multiple directions, they can overcome the problems of the GLDM, GLRLM and SGLDM methods, whose performances depend on extraction directions. Furthermore, extracting features in multiple directions enables the proposed method to obtain richer information from the image than those methods using only one direction.

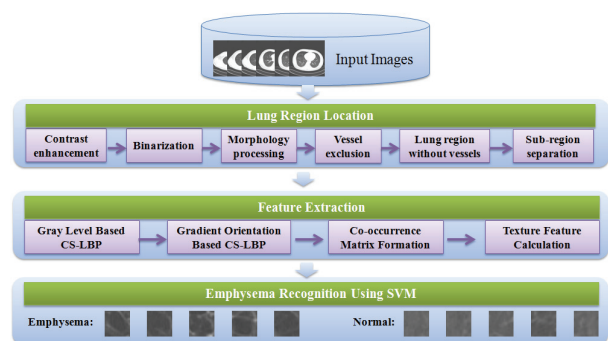


Fig. 2. The CAD system for emphysema recognition

Based on these new texture features, a CAD system for emphysema detection is presented in this

paper. As shown in Fig. 2, the lung region is first located by contrast enhancement, binarization, morphological processing, and vessel exclusion (these steps are detailed in Section 3). Then, the pure lung region is separated into sub-regions and the proposed method is applied to extract texture features. Finally, the support vector machine is used to recognize the emphysema regions.

Major points of this paper are:

- New brightness and structural uniformity texture features based on CS-LBP can represent the image's local brightness and structure characteristics.
- New texture features that are extracted in multiple directions contain richer information than those of GLDM, GLRLM, and SGLMD.

2. Related works

SGLDM has been widely used in medical image analysis [12–14]. This method is based on the assumption that the texture-context information in an image is contained in the overall spatial relationship that the gray level goes from one to another [15]. It derives texture features by means of the spatial distribution of pairs of gray levels having certain distance and orientation. This method estimates the second order joint conditional probability density function $f(i, j | d, \theta)$. Each $f(i, j | d, \theta)$ is the probability of going from gray level i to gray level j with an inter-sample space d and a direction θ , where θ is usually 0, 45, 90, and 135 degrees [3]. For a given image where the gray level is L , for example, a matrix $L \times L$ based on $f(i, j | d, \theta)$ can be constructed. Texture features, such as “Variance”, “Difference variance”, “Sum entropy”, “Difference Entropy”, and “Entropy” are then extracted from the matrix.

GLRLM [9] is based on computing the number of gray level runs of various lengths. In GLRLM [13], the gray level run is a set of linearly adjacent pixels in the image that have the same gray values. The length of the run is the number of pixels having the same gray values within the run. The element $r'(i, j | \theta)$ of the gray level run length matrix is defined as follows:

$$R(\theta) = [r'(i, j | \theta)] \quad (1)$$

This element specifies the estimated number of times an image contains a run of length j , for gray level i , in the direction of angle θ [16]. Five kinds of texture features are defined based on the gray level run length matrix (short runs emphasis, long runs emphasis, gray level non-uniformity, run length non-uniformity, run percentage) for describing the image characteristics.

The GLDM [8] is based on the absolute differences between pairs of gray levels in an image. Let $I(x, y)$ be the image intensity function. Then for any given displacement $\delta = (\Delta x, \Delta y)$, we can calculate the absolute gray level difference between this pair, i.e.,

$$D_\delta(x, y) = |I(x, y) - (I(x + \Delta x, y + \Delta y))| \quad (2)$$

Let $f'(\cdot | \delta)$ be the estimated probability density function associated with the possible values of D_δ , i.e.,

$$f'(i | \delta) = P(D_\delta(x, y) = i) \quad (3)$$

Based on the probability density function, five texture features (contrast, angular second moment, entropy, mean, inverse difference moment) are

defined [16].

The LBP operator, which was first introduced by Harwood et al. [9], generates binary codes by establishing relationships of 3-by-3 neighboring pixels with the center pixel value. It generates a binary code 0 if the value of the neighbor pixel is smaller than that of the center pixel. Otherwise, it generates a binary code 1. These binary codes are then multiplied with corresponding weights and the results are then summed up to generate an LBP code. Fig. 3 shows the process generating an LBP code.

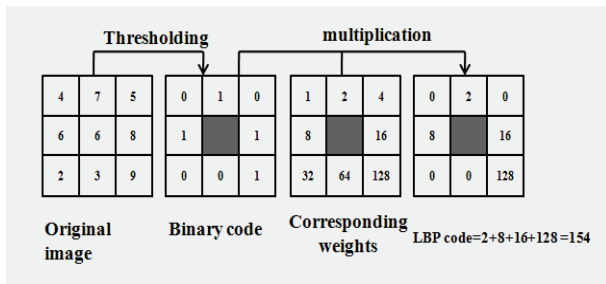


Fig. 3. The process of calculating the LBP code

The original LBP was then extended to derive from a circular symmetric neighbor set of N members on a circular region with radius R [10]. The interpolation method is applied to calculate the gray value of the neighboring pixels which do not fall exactly in the pixel position. It is calculated as follows:

$$LBP_{N,R}(x_c, y_c) = \sum_{n=0}^{N-1} s(g_n - g_c) 2^n \quad (4)$$

where (x_c, y_c) is the position of the center point, g_c is the pixel value of the center point, while g_n is the pixel value of the neighboring pixel, and:

$$s(g_n - g_c) = \begin{cases} 1 & g_n \geq g_c \\ 0 & g_n < g_c \end{cases} \quad (5)$$

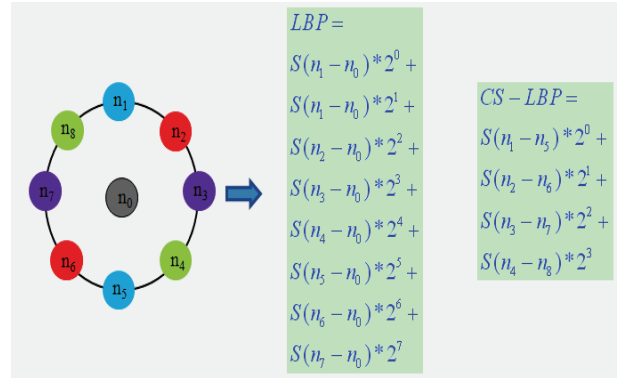


Fig. 4. LBP and CS-LBP codes for a neighborhood of 8 pixels

Recently, the Center-Symmetric Local Binary Pattern (CS-LBP), a modified version of LBP, was proposed to represent the image texture features. Compared with LBP, CS-LBP requires half the number of comparisons for the same number of neighbors by comparing center-symmetric pairs of pixels (Fig. 4). The CS-LBP code is calculated as follows:

$$CS-LBP_{R,N,T}(x,y) = \sum_{i=0}^{(N/2)-1} s[n_i - n_{i+(N/2)}] * 2^i, \quad s(x) = \begin{cases} 1, & x > T \\ 0, & x \leq T \end{cases} \quad (6)$$

where R is the radius of the circular region, N is the number of neighboring pixels, T is a threshold and n_i and $n_{i+(N/2)}$ correspond to the gray values of center symmetric pairs of pixels. Robustness on flat image regions can be obtained by establishing relationships between the gray level differences and a small value T .

3. Lung region location

To detect the emphysema regions in the CT images, the lung region without vessels must be located. The process of locating the lung region is shown in Fig. 5.

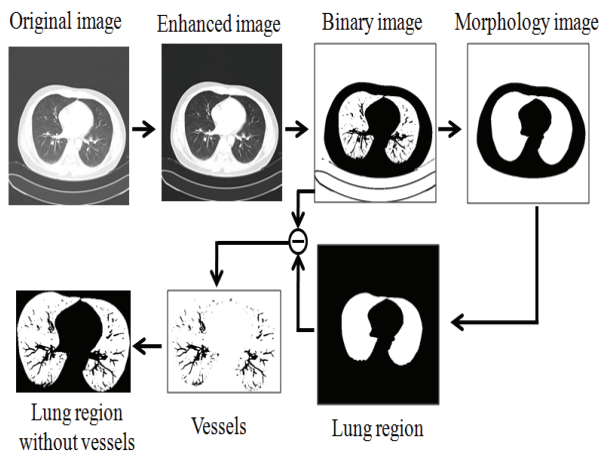


Fig. 5. The processing of lung region location

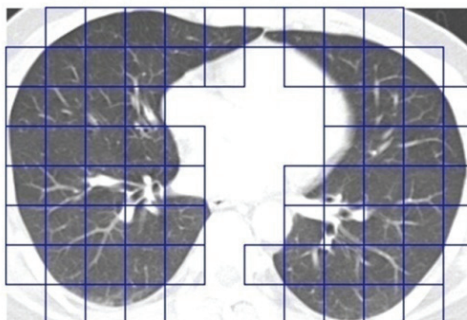


Fig. 6. Sub-regions of the lung image

First, the contrast of the original CT image is enhanced by *gamma correction* [5]. Then, the Otsu method [17] is employed to obtain a binary image, and the morphological processing (Open) is applied to remove the noise and vessels in the binary image. Therefore, the lung region can be located by growing the region in the “opened” image. The lung vessels are then detected by subtracting the lung region from the binary image, and finally the lung region without vessels is obtained.

In the next step, the lung region without vessels is separated into 30-by-30 sub-regions as Liang *et al.* [5] did (Fig. 6). The sub-regions that cover more than 70[%] of the lung will be calculated during the texture feature extraction [5].

4. Proposed method

Feature extraction is a very important step for emphysema recognition. The emphysema regions in the CT images are found with some essentially local structural and brightness characteristics. As shown in Fig. 7, the emphysema region is darker than the normal region and its surface is smooth. Therefore, features that are extracted from the image regions are required to present the brightness and structural characteristics of the image well. For this purpose, in this paper, we propose to use the gray level based CS-LBP and gradient orientation difference based CS-LBP to estimate the uniformity of the image brightness and structure.

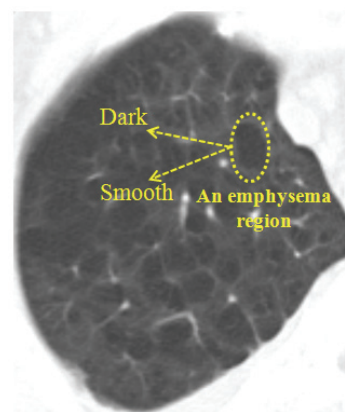


Fig. 7. An example of emphysema region

As described in Section 2, the CS-LBP is a good measure for the flatness of an image. We propose to use the CS-LBP to estimate the brightness uniformity of the image. However, the CS-LBP fails to estimate the structural uniformity of the image. Fig. 8 (a) and (b) represent two 3-by-3 regions. Both image regions can generate the same CS-LBP codes ($T=2$) whereas their structures are different.

Numerals in Fig. 8 (a) and (b) below denote the gray value of the pixels.

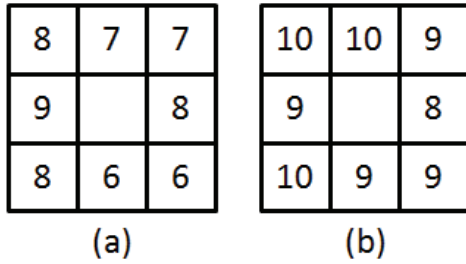


Fig. 8. An example of two image regions

To overcome this problem and further estimate the local structures, we propose to calculate the gradient orientation difference between the center-symmetric pairs in order to estimate the similarity of the image structure. As shown in Fig. 9, the gradient orientation of each point in the image region is first calculated. Then, the gradient orientation differences between the symmetric pairs can be obtained. Finally, another CS-LBP code can be generated based on the gradient orientation differences.

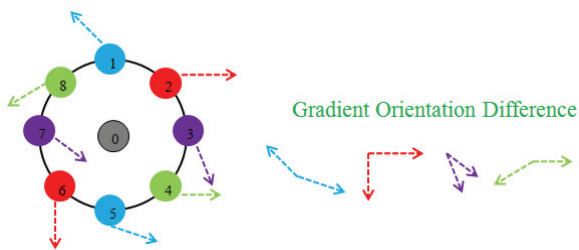


Fig. 9. Calculation of the gradient orientation difference

The gradient orientation is calculated as follows:

$$O_{\theta}(x, y) = \tan^{-1} \left(\frac{I(x, y+1) - I(x, y-1)}{I(x+1, y) - I(x-1, y)} \right) \quad (7)$$

where $I(x, y)$ is the gray value of the pixel in position of (x, y) . Therefore, the gradient orientation difference is calculated by:

$$GOD(x, y)_{x_i, y_i} = |O_{\theta}(x_i, y_i) - O_{\theta}(x_{i+N/2}, y_{i+N/2})| \quad (1 \leq i \leq N/2) \quad (8)$$

where N is the number of neighboring pixels around the position (x, y) . Finally, another CS-LBP code is generated based on the gradient orientation difference:

$$CS-LBP_{R,N,T_{\theta}}^{GOD}(x, y) = \sum_{i=0}^{N-1} S(GOD)2^i, \quad s(x) = \begin{cases} 1, & x \geq T_{\theta} \\ 0, & \text{otherwise} \end{cases} \quad (9)$$

where T_{θ} is a threshold for the gradient orientation similarity and R is the radius.

Two CS-LBP codes that can describe the brightness and structural uniformity are obtained for a pixel in the image. As mentioned earlier, the gray value is also an important factor since the emphysema regions are darker than their backgrounds. Based on this, we propose to generate a pair of values for each pixel by combining the gray value and both CS-LBP codes. The pair values are calculated as follows:

$$V(x, y)_{R,N,T} = \begin{cases} V_1 = I(x, y) * \frac{CS-LBP_{R,N,T}}{2^{N/2}} \\ V_2 = I(x, y) * \frac{CS-LBP_{R,N,T_{\theta}}^{GOD}}{2^{N/2}} \end{cases} \quad (10)$$

As shown in (10), the gray value is degraded by both CS-LBP codes. Since both values are obtained in multiple directions, valuable information is extracted. A region with flat brightness and similar structures will have lower values and thus the features based on these values can be more distinctive.

From the pairs of values generated by both CS-LBP codes, we can define a conditional probability density function $F(V_1, V_2 | N, R)$ based on (10), where $0 \leq V_1 < L$ and $0 \leq V_2 < L$ (suppose the

gray level range is 0~L). A matrix with size of $L*L$ based on the function $F(V_1, V_2|N, R)$ is obtained as follows:

$$M(V_1, V_2|N, R) = \begin{bmatrix} F(0,0|N, R) & F(0,1|N, R) & \dots & F(0,L|N, R) \\ F(1,0|N, R) & F(1,1|N, R) & \dots & F(1,L|N, R) \\ \vdots & \vdots & \ddots & \vdots \\ F(L,0|N, R) & F(L,1|N, R) & \dots & F(L,L|N, R) \end{bmatrix} \quad (11)$$

Finally, five texture features are defined to represent the characteristics of the image.

1. Entropy:

$$ENT = - \sum_{l=0}^{L-1} \sum_{d=0}^{L-1} F(l, d | N, R) \log [F(l, d | N, R)] \quad (12)$$

2. Brightness Variance Emphasis (BVE):

$$BVE = \sum_{l=0}^{L-1} \sum_{d=0}^{L-1} F(l, d | N, R) * (l+1) \quad (13)$$

3. Brightness Uniformity Emphasis (BUE):

$$BUE = \sum_{l=0}^{L-1} \sum_{d=0}^{L-1} \frac{F(l, d | N, R)}{l+1} \quad (14)$$

4. Structure Variance Emphasis (SVE):

$$SVE = \sum_{l=0}^{L-1} \sum_{d=0}^{L-1} F(l, d | N, R) * (d+1) \quad (15)$$

5. Structure Uniformity Emphasis

$$SUE = \sum_{l=0}^{L-1} \sum_{d=0}^{L-1} \frac{F(l, d | N, R)}{(1+d)} \quad (16)$$

Among these features, entropy provides an indication of the complexity within an image; a complex image has a high entropy value [18]. The BVE and BUE can be measures of the brightness and its uniformity, while SVE and SUE are measures of structural uniformity of an image.

5. Experimental result

5.1 Data collection

Two kinds of emphysema, centrilobular emphysema (CLE) and panlobular emphysema (PLE) were used to test the performance of the proposed method. The following experiments used 339 CLE images and 492 PLE images. These images were captured with 5[mm] slice and a resolution of

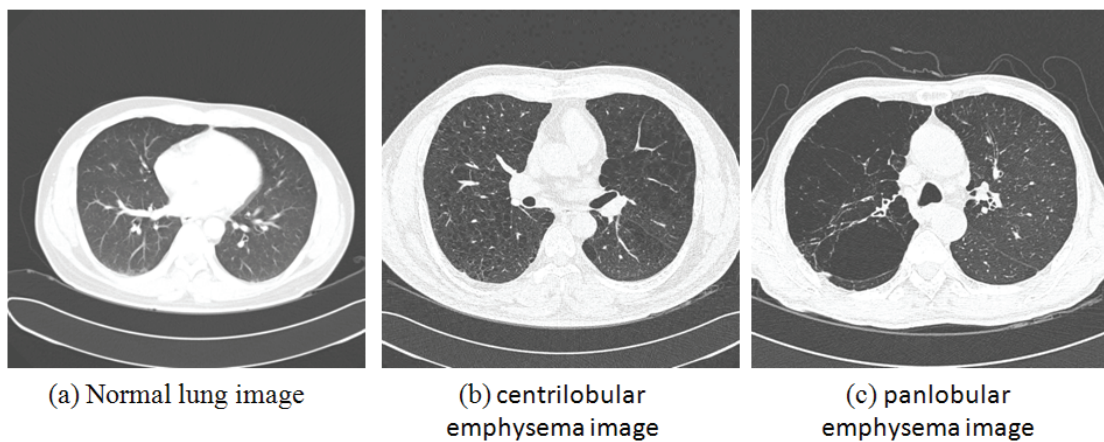


Fig. 10. The experimental image samples

1024*1024. All the images were stored in BMP format with 8 bits. Fig. 10 (a) is a normal lung image while (b) and (c) show the visual characteristics of both CLE and PLE.

Centrilobular emphysema (Fig. 10 (b)) appears as focal areas of a low-attenuation lung within a homogeneous background of normal lung parenchyma. The panlobular emphysema (Fig. 10 (c)) appears as large and extensive areas of uniform low attenuation.

The images were then processed as mentioned in Section 3. First the lung regions without vessels were located and the sub-regions were obtained. Texture features were then extracted from the sub-regions covering more than 70[%] of the lung. 1,800 sub-regions were collected for the performance evaluation, including 600 normal sub-regions, 600 CLE sub-regions and 600 PLE sub-regions. For each class, 100 sub-regions were used to train the classifier. The remaining 500 sub-regions were used for performance testing.

5.2 Performance evaluation

The proposed method was evaluated by comparing its sensitivity, specificity, accuracy and ROC curves with those of SGLDM, GLRLM and GLDM. We defined the True Positive, True Negative, False Positive, and False Negative as follows:

True positive (TP): number of emphysema sub-regions correctly classified.

True negative (TN): number of normal sub-regions correctly classified.

False positive (FP): number of normal sub-regions incorrectly classified as emphysema regions.

False negative (FN): number of emphysema sub-regions incorrectly classified as normal regions.

The Sensitivity, Specificity, and Accuracy are then defined as follows:

$$sensitivity(\%) = \frac{TP}{TP + FN} * 100 \quad (38)$$

$$specificity(\%) = \frac{TN}{FP + TN} * 100 \quad (39)$$

$$accuracy(\%) = \frac{TP + TN}{TP + FN + FP + TN} * 100 \quad (40)$$

For a fair comparison, five texture features for each method (SGLDM, GLRLM, GLDM and the proposed method) were used as feature vectors. Table 1 shows the texture features for each method. Since the SGLDM, GLRLM and GLDM methods are symmetric in directions, we extracted the texture features using four directions: 0, 45, 90, and 135 degrees. The inner distances for SGLDM and GLDM were set at 1 which provided the best result for both methods.

For the proposed method, the best result was achieved by setting the number of neighboring pixels at 8, the radius at 2, the threshold T at 4 for V_1 and the threshold T_θ at 30 degrees for V_2 . Since the support vector machine (SVM) has been used as an effective method for pattern recognition and it has demonstrated good performance in CAD systems [19,20], it was applied to our system for emphysema recognition.

Table 2 compares the results of the proposed method and SGLDM. Since the proposed method extracted features based on the local brightness and structural uniformity in multiple directions, we see the proposed method performs better than the SGLDM with respect to the sensitivity, specificity and accuracy for both CLE and PLE. The results show that the performance of SGLMD depends on the feature extraction directions. The SGLMD

showed its lowest performance for CLE and PLE in the direction of 45 and 0 degrees, respectively. Compared to the SGLDM, the proposed method

achieved higher sensitivity and accuracy for both CLE and PLE.

Table 3 compares the results of the proposed

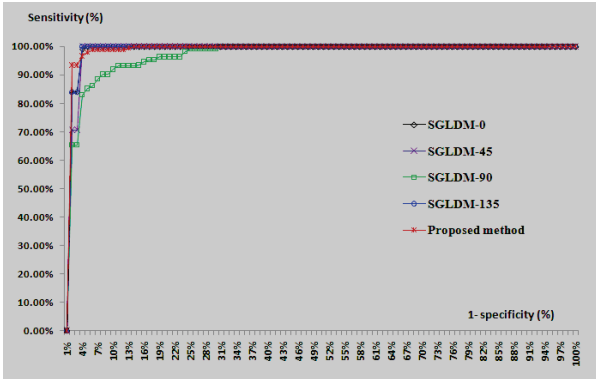


Fig. 11. The CLE ROC curves of the proposed method and SGLDM

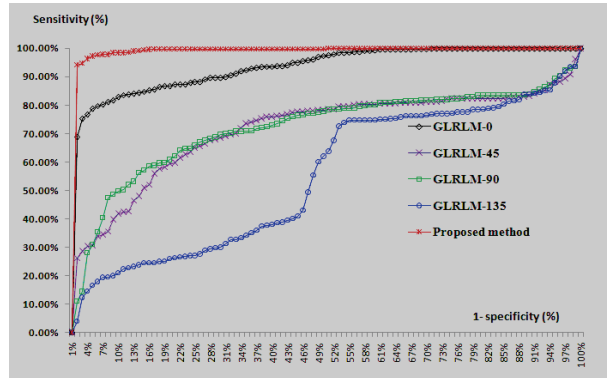


Fig. 14. The PLE ROC curves of the proposed method and GLRLM

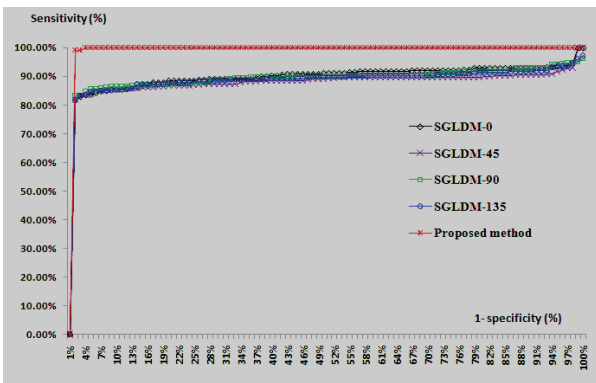


Fig. 12. The PLE ROC curves of the proposed method and SGLDM

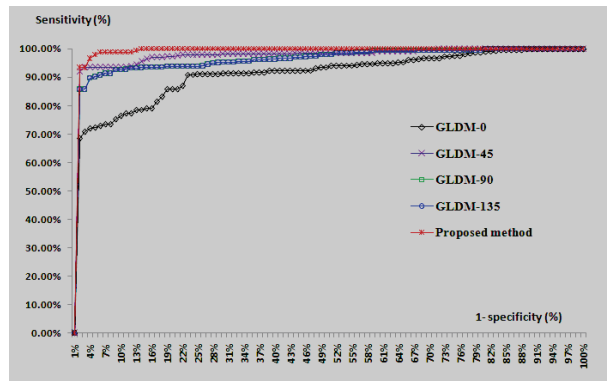


Fig. 15. The CLE ROC curves of the proposed method and GLDM

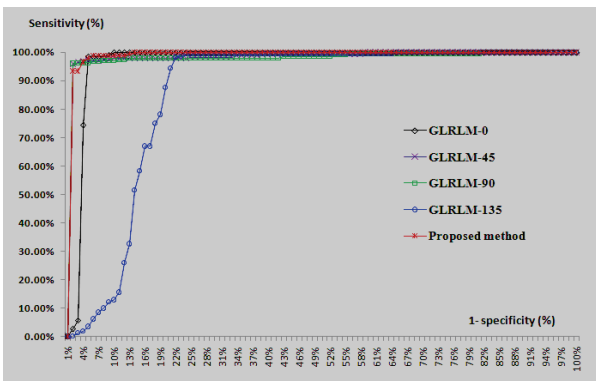


Fig. 13. The CLE ROC curves of the proposed method and GLRLM

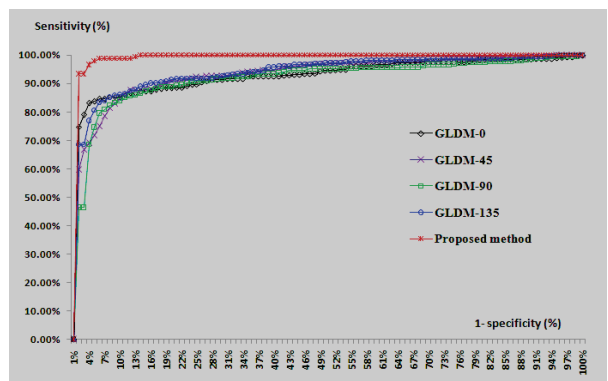


Fig. 16. The PLE ROC curves of the proposed method and GLDM

method and GLRLM. Similar to the SGLDM, the results of GLRLM also depend on the feature extraction directions. For the case of PLE, the

GLRLM showed low performance with respect to Specificity and it showed its lowest result in the direction of 135 degrees. For both CLE and PLE, the

Table 1. Texture features for each method

Method	Features				
Proposed method	Entropy	BVE	BUE	SVE	SUE
SGLDM	Entropy	Variance	Difference variance	Sum entropy	Difference Entropy
GLRLM	short runs emphasis	long runs emphasis	gray level non-uniformity	run length non-uniformity	run percentage
GLDM	entropy	Contrast	angular second moment	mean	inverse difference moment

Table 2. The performance of the proposed method vs. SGLDM

Disease	Results	Proposed method	SGLDM 0 degree	SGLDM 45 degrees	SGLDM 90 degrees	SGLDM 135 degrees
CLE	Sensitivity ([%])	93.00	84.20	69.40	86.20	82.40
	Specificity ([%])	98.80	97.80	99.80	95.20	99.80
	Accuracy ([%])	95.90	91.00	84.60	90.70	91.10
PLE	Sensitivity ([%])	94.60	73.20	76.20	75.80	75.20
	Specificity ([%])	98.60	99.80	99.80	99.80	99.80
	Accuracy ([%])	96.60	86.50	88.00	87.80	87.50

Table 3. The performance of the proposed method vs. GLRLM

Disease	Results	Proposed method	GLRLM 0 degree	GLRLM 45 degrees	GLRLM 90 degrees	GLRLM 135 degrees
CLE	Sensitivity ([%])	93.00	100.00	98.80	98.00	99.40
	Specificity ([%])	98.80	81.00	64.80	80.60	62.00
	Accuracy ([%])	95.90	90.50	81.80	89.30	80.70
PLE	Sensitivity ([%])	94.60	85.20	80.60	79.60	76.20
	Specificity ([%])	98.60	85.60	38.00	43.60	32.60
	Accuracy ([%])	96.60	85.40	59.30	61.60	54.40

Table 4. The performance of the proposed method vs. GLDM

Disease	Results	Proposed method	GLRLM 0 degree	GLRLM 45 degrees	GLRLM 90 degrees	GLRLM 135 degrees
CLE	Sensitivity ([%])	93.00	91.40	98.40	99.40	98.00
	Specificity ([%])	98.80	65.40	57.80	38.00	52.60
	Accuracy ([%])	95.90	78.40	78.10	68.70	75.30
PLE	Sensitivity ([%])	94.60	60.20	71.60	87.60	91.60
	Specificity ([%])	98.60	99.80	96.60	85.00	79.80
	Accuracy ([%])	96.60	80.00	84.10	86.30	85.70

proposed method achieved its best result with respect to Specificity and Accuracy.

Table 4 compares the results of the proposed method and GLDM. Since the proposed method extracted more feature information than the GLMD, it outperformed the GLDM in both cases of CLE and PLE. The GLDM showed low specificity in the case of CLE and low sensitivity in the case of PLE. Its performance depended on the feature extraction directions. Comparing the accuracy of the proposed method with the average accuracy of the GLDM in 0 degree, 45 degrees, 90 degrees and 135 degrees directions, the proposed method achieved 20.77[%] and 12.57[%] higher accuracy in the cases of CLE and PLE, respectively.

Receiver Operating Characteristic (ROC) curves of the proposed method and SGLDM, GLRLM, GLDM for the cases of CLE and PLE are shown in Fig. 11~16. The ROC curve plots the true positive rate against the false positive rate (1-specificity) of a diagnostic test. The tradeoff between sensitivity and specificity is shown. In theory, the area under the curve is a measure of test accuracy.

As seen on Fig. 11~16, the y-axis denotes the true positive rate, while the x-axis denotes the false positive rate. It is clear that a good diagnosis result can give a high true positive rate while keeping the false positive rate low.

Therefore, the closer the curve follows the left-hand border and the top border of the ROC space, the more accurate the test is. As seen in Fig. 14, comparing the ROC curve of the proposed method with those of GLRLM for the case of PLE, the proposed method greatly outperformed the GLRLM. Observing from Fig. 11~16, we find that the ROC curve of the proposed method is closer to the left-top than those of SGLDM, GLRLM and GLDM in all cases. Therefore, the proposed method has better distinguishing ability than those of

SGLDM, GLRLM and GLDM.

6. Conclusion

A new texture feature extraction method based on brightness and structural uniformity estimation is proposed in this paper. By taking advantage of the CS-LBP and gradient orientation differences, the proposed method estimates the image brightness and structural uniformity in multiple directions. Thereby, more rich and distinctive feature information can be extracted by the proposed method. Based on the combination of the gray level, CS-LBP, and gradient orientation differences, the proposed method is able to better distinguish the emphysema regions than the SGLMD, GLRLM and GLDM with respect to the sensitivity, specificity, and accuracy.

In future work, the fuzzy based CS-LBP will be used with the proposed feature extraction system so as to improve the performance of the proposed method. This method will be applied to other detections of lesion regions in CT images, such as honeycombing, and bronchiolitis obliterans.

The present research was conducted by the research fund of Dankook University in 2010

References

- [1] M. Park, B. Kang, S.J. Jin, and S. Luo, Computer Aided Diagnosis System of Medical Images using Incremental Learning Method, *Expert Systems with Applications*, volume 36, pages 7242-7251, 2009.
- [2] A. M. R. Schilham, B. V. Ginneken, and M. Loog, A Computer-Aided Diagnosis System for Detection of Lung Nodules in Chest Radiographs with an Evaluation on a Public Database, *Medical Image Analysis*, volume 10, pages 247-258, 2006.
- [3] K. Takei, N. Homma, T. Ishibashi, M. Sakai, and M. Yoshizawa, Computer Aided Diagnosis for Pulmonary Nodules by Shape Feature Extraction, In: *SICE Annual*

- Conference 2007, Kagawa University, Takamatsu City, Japan, September 17-20, pages 1964-1967, 2007.
- [4] H. Zhang, J. E. Fritts, and S. A. Goldman, A Fast Texture Feature Extraction Method for Region-based Image Segmentation, *Image and video communications and processing*, volume 5685 (2), pages 957-968, 2005.
- [5] T. K. Liang, T. Tanaka, H. Nakamura and A. Ishizaka, A Neural Network based Computer-Aided Diagnosis of Emphysema using CT Lung Images, In: *SICE Annual Conference 2007*, Kagawa University, Takamatsu City, Japan, September 17-20, pages 703-709, 2007.
- [6] Shao-Hu Peng, Deok-Hwan Kim, Seok-Lyong Lee, Myung-Kwan Lim, Texture Feature Extraction Based on a Uniformity Estimation Method for Local Brightness and Structure in Chest CT Images, *Computers in Biology and Medicine*, in press, 2010.
- [7] Shao-Hu Peng, Khairul Muzzammil, and Deok-Hwan Kim, Quantitative Image Analysis of Chest CT Using Gray Level Local Binary Pattern Texture Feature, *ICCC 2009*, 2009-12-18 pp.129-132.
- [8] A. H. Mir, M. Hanmandlu and S.N. Tandon, Texture Analysis of CT Images, In: *Engineering in Medicine and Biology Magazine*, IEEE, volume 14, pages 781-786, 1995.
- [9] T. Ojala, M. Pietikainen, and D. Harwood, A Comparative Study of Texture Measures with Classification Based on Feature Distributions, *Pattern recognition*, volume 29, pages 51-59, 1996.
- [10] T. Ojala, M. Pietikainen, and T. Maenpaa, Multiresolution Gray-Scale and Rotation Invariant Texture Classification with Local Binary Patterns, *IEEE Transactions on Pattern Analysis and Machine Intelligence*, volume. 24, No. 7, pages 971 -987, 2002.
- [11] Marko Heikkila, Matti Pietikainen, Cordelia Schmid, Description of interest regions with local binary patterns, *Pattern Recognition*, Vol.42, pp.425-436, 2009.
- [12] T. Glatard, J. Montagnat, and I. E. Magnin, Texture Based Medical Image Indexing and Retrieval: Application to Cardiac Imaging, In: *the 6th ACM SIGMM international workshop on Multimedia information retrieval*, New York, USA, October 15-16, pages 135-142, 2004.
- [13] I. Valavanis, S. G. Mouggiakakou, K. S. Nikita, and A. Nikita, Computer Aided Diagnosis of CT Focal Liver Lesions by an Ensemble of Neural Network and Statistical Classifiers, In: *2004 IEEE International Joint Conference on Neural Networks*, Budapest, Hungary, July 25-29, volume 3, pages 1929- 1934, 2004.
- [14] W. L. Zhang and X. Z. Wang, Feature Extraction and Classification for Human Brain CT Image, In: *the Sixth International Conference on Machine Learning and Cybernetics*, Hong Kong, August 19-22, volume 2, pages 1155-1159, 2007.
- [15] R. M. Haralick, K. Shanmugam and I. Dinstein, Textural Features for Image Classification, *IEEE Transactions on System, Man, and Cybernetics*, volume SMC-3, pages 610-621, 1973.
- [16] R. W. Conners, and C.A.Harlow, A Theoretical Comparison of Texture Algorithms, *IEEE Transactions: Pattern Analysis and Machine Intelligence*, pp. 204-222, 1980.
- [17] N. Otsu, A Threshold Selection Method from Gray-Level Histogram, *IEEE Transactions on System Man Cybernetics*, volume SMC-9, No.1, pages 62-66, 1979.
- [18] B. Park, Y. R. Chen, Co-occurrence Matrix Texture Features of Multi-spectral Images on Poultry Carcasses, *Journal of Agricultural Engineering Research*, Volume 78, Issue 2, Pages 127-139, 2001.
- [19] A. Shamsheyeva, A. Shamsheyeva, The Anisotropic Gaussian Kernel for SVM classification of HRCT images of the lung, in: *Intelligent Sensors, Sensor Networks and Information Processing Conference*, pp. 439-444, 2004.
- [20] R. F. Chang, W. J Wu, W. K. Moon, Y. H Chou and D. R. Chen, Support Vector Machines for Diagnosis of Breast Tumors on US Images, *Academic Radiology*, Vol. 10, pp. 189-197, 2003.

Biography



Shao-Hu Peng

Shao-hu Peng received B.S. and M.S degrees from Guangdong University of Technology in 2005, 2007, respectively. Since Sep. 2010, He has been a Ph. D. student at School of Electronic and Electrical Engineering in Dankook University. His major research interests include image processing and adaptive signal processing.



Hyun-Do Nam

Hyun Do Nam received B.S., M.S and Ph.D. degrees from Seoul National University in 1979, 1981, 1986, respectively. Since Mar. 1982, He has been with Dankook University as a professor at School of Electronic and Electrical Engineering. His major research interests include digital signal processing and active noise control.